

THE OFFICIAL MAGAZINE OF THE OCEANOGRAPHY SOCIETY

Oceanography

CITATION

Hormann, V., L.R. Centurioni, A. Mahadevan, S. Essink, E.A. D'Asaro, and B. Praveen Kumar. 2016. Variability of near-surface circulation and sea surface salinity observed from Lagrangian drifters in the northern Bay of Bengal during the waning 2015 southwest monsoon. *Oceanography* 29(2):124–133, <http://dx.doi.org/10.5670/oceanog.2016.45>.

DOI

<http://dx.doi.org/10.5670/oceanog.2016.45>

COPYRIGHT

This article has been published in *Oceanography*, Volume 29, Number 2, a quarterly journal of The Oceanography Society. Copyright 2016 by The Oceanography Society. All rights reserved.

USAGE

Permission is granted to copy this article for use in teaching and research. Republication, systematic reproduction, or collective redistribution of any portion of this article by photocopy machine, reposting, or other means is permitted only with the approval of The Oceanography Society. Send all correspondence to: info@tos.org or The Oceanography Society, PO Box 1931, Rockville, MD 20849-1931, USA.

Variability of Near-Surface Circulation and Sea Surface Salinity Observed from Lagrangian Drifters in the Northern Bay of Bengal During the Waning 2015 Southwest Monsoon

By Verena Hormann, Luca R. Centurioni,
Amala Mahadevan, Sebastian Essink,
Eric A. D'Asaro, and B. Praveen Kumar

Photo credit:
Gualtiero
Spiro Jaeger

“ This study focuses on a major observational effort in the northern bay during the waning 2015 southwest monsoon, where a large array of Surface Velocity Program (SVP) drifters drogued at 15 m depth and equipped with salinity and/or temperature sensors was deployed as part of the ASIRI program. ”

ABSTRACT. A dedicated drifter experiment was conducted in the northern Bay of Bengal during the 2015 waning southwest monsoon. To sample a variety of spatiotemporal scales, a total of 36 salinity drifters and 10 standard drifters were deployed in a tight array across a freshwater front. The salinity drifters carried for the first time a revised sensor algorithm, and its performance during the 2015 field experiment is very encouraging for future efforts. Most of the drifters were quickly entrained in a mesoscale feature centered at about 16.5°N, 89°E and stayed close together during the first month of observations. While the eddy was associated with rather homogeneous temperature and salinity characteristics, much larger variability was found outside of it toward the coastline, and some of the observed salinity patches had amplitudes in excess of 1.5 psu. To particularly quantify the smaller spatiotemporal scales, an autocorrelation analysis of the drifter salinities for the first two deployment days was performed, indicating not only spatial scales of less than 5 km but also temporal variations of the order of a few hours. The hydrographic measurements were complemented by first estimates of kinematic properties from the drifter clusters, however, more work is needed to link the different observed characteristics.

INTRODUCTION

The South Asian monsoon dominates the climate of the Indian Ocean region, drastically affecting life on the Indian subcontinent (e.g., Bhat et al., 2001; Gadgil, 2003). This emphasizes the great importance of understanding and predicting the monsoon and its variability accurately. The Air-Sea Interactions Regional Initiative (ASIRI) is designed to improve present knowledge of coupled ocean-atmosphere interactions in the region (Lucas et al., 2014; Wijesekera et al., in press). This research effort focuses on the Bay of Bengal (BoB) since most of the monsoon rainfall arises from synoptic (low-pressure) weather systems that especially develop over the warm waters

of the bay. The upper ocean is affected not only by large freshwater input from rainfall but also by major river run-offs. Monsoon-driven reversals of the seasonal circulation (e.g., Schott and McCreary, 2001) challenge the quantification of regional air-sea processes, and significant gaps remain in current understanding. A priority of ASIRI has been to better determine upper-ocean freshwater budgets, including mixing and advection, since shallow salinity-controlled mixed layers impact the heat distribution in the near-surface layer (e.g., Shenoi et al., 2002; Rao and Sivakumar, 2003). While the basin-scale circulation and associated salinity advection are primarily wind-driven, the monsoonal

forcing also generates energetic meso- and submesoscale features (e.g., Lucas et al., 2014). Quantifying the dominant processes on these smaller scales has been a compelling objective of ASIRI, in particular with regard to improving monsoon predictions by numerical models that require a better understanding of the spatiotemporal variability in the BoB for more accurate parameterizations of the relevant physics.

This study focuses on a major observational effort in the northern bay during the waning 2015 southwest monsoon (Figure 1a), where a large array of Surface Velocity Program (SVP) drifters drogued at 15 m depth and equipped with salinity and/or temperature sensors was deployed as part of the ASIRI program. Earlier drifter deployments within the framework of ASIRI occurred primarily off the coast of Sri Lanka to address another program objective concerned with the coastal boundary currents and exchanges between the BoB and the Arabian Sea (Wijesekera et al., 2015, in press; Lee et al., 2016, in this issue). In addition to describing the 2015 field experiment and performance of the salinity drifters (SVP-S) in particular, this article provides first insights into the observed variability on multiple spatiotemporal scales and processes influencing the variability of surface salinity in the BoB such as horizontal stirring.

2015 DRIFTER EXPERIMENT

The drifter experiment in the northern BoB during the most recent field campaign in August–September 2015 was designed to sample a variety of spatio-temporal scales, and particularly the horizontal advection of freshwater as the drifters disperse. Most of the annual freshwater input occurs during the southwest monsoon season between June and September (e.g., Bhat et al., 2001; Gadgil, 2003), which provides an optimal

background for detailed measurements of upper-ocean processes that govern the heat and salt budgets.

Satellite altimetry indicated that meso-scale eddies characterized the surface flow field in the northern bay during the first month of the 2015 drifter experiment described herein (Figure 1b). The thickness of the fresh layer (i.e., <30 psu) can be just 5–10 m in the deployment region of the drifter array as revealed by salinity measurements recorded by a Lagrangian

float (D'Asaro, 2003) deployed near an SVP-S drifter pair from a concurrent Indian research cruise on OSV *Sagar Nidhi* (Figure 2). During its week-long deployment, the profiling float generally followed the drifters, and the lowest near-surface salinities were observed in the last two days of the record when the float was moving southwestward.

A total of 36 SVP-S (e.g., Reverdin et al., 2007; Hormann et al., 2015) and 10 SVP (e.g., Niiler, 2001; Maximenko et al., 2013) drifters were deployed in a tight array across an identified freshwater front in international waters from R/V *Roger Revelle* at the beginning of September 2015 (Figure 2a). In order to also resolve smaller-scale features in space and time, the salinity drifters were initially programmed to transmit their parameters every five (instead of 30) minutes. The array was largely organized in clusters consisting of three SVP-S drifters plus one SVP drifter (i.e., ~5 min apart), with most deployments on the fresher side of the salinity front. The reason for the additional deployment of standard SVP drifters was to improve the overall representation of the surface circulation in the BoB where observations of ocean currents are lacking.

SVP-type drifters using the Argos or Iridium satellite systems for data transmission are designed to follow the water at 15 m depth in a Lagrangian sense, and velocity measurements are accurate to within 0.01 m s^{-1} for winds up to 10 m s^{-1} (Niiler, 2001; Maximenko et al., 2013). Here, the drifter velocities were estimated from first-order central differences of the position information obtained by GPS fixes, which were quality controlled by applying a three-point median filter. In addition to ocean currents, the SVP drifters measure sea surface temperature at a depth of a few centimeters below the surface with an accuracy of $\pm 0.1^\circ\text{C}$. The deployed SVP-S drifters were each equipped with a Sea-Bird Electronics SBE37-SI sensor (accuracy: 0.0003 S m^{-1} for conductivity or $\sim 0.003 \text{ psu}$ for salinity, and 0.002°C

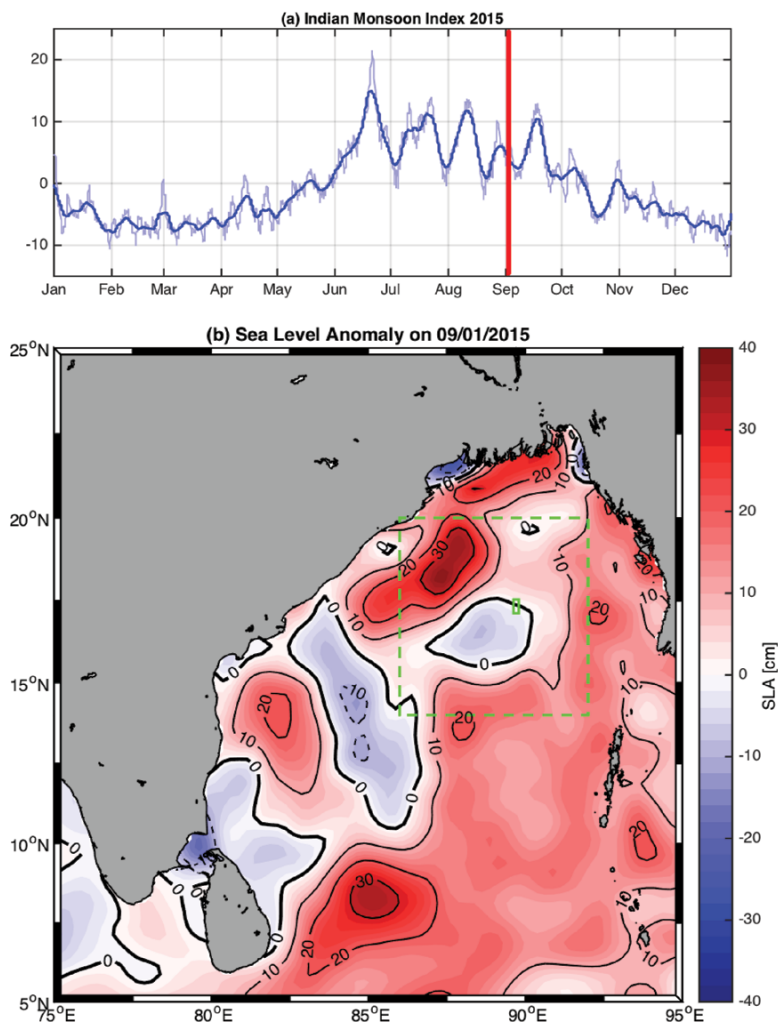


FIGURE 1. (a) Indian monsoon index in 2015 (Wang and Fan, 1999; Wang et al., 2001) using ERA-Interim winds (Dee et al., 2011), with six-hour data shown in light blue and the corresponding seven-day running mean in darker blue. The red line marks the drifter deployments during an R/V *Roger Revelle* cruise at the beginning of September. (b) Map of near-real-time sea level anomalies (black contours in intervals of 10 cm) from the Copernicus Marine Environment Monitoring Service (CMEMS) on September 1, 2015 (Ducet et al., 2000), that is, immediately before the beginning of the drifter deployments, with the corresponding region marked by the small green box with the solid outline. The much larger dashed green box indicates the area covered by the drifters during the first month of observations (cf. Figure 4).

for temperature) located just underneath the surface buoy at an approximate depth of 0.5 m (e.g., Centurioni et al., 2015; Hormann et al., 2015). The presence of the drogue is detected with a strain gauge installed inside the drifter's hull and near the tether's attachment. All drifter drogues remained attached through the end of the first month discussed here.

SVP-S PERFORMANCE

During the first Salinity Processes in the Upper-ocean Regional Study (SPURS-1) in the subtropical North Atlantic, a flaw in the algorithm used for the onboard computation of satellite-transmitted drifter salinities was discovered that introduced a predominantly fresh bias in the noise level of the data (Centurioni et al., 2015; Hormann et al., 2015). A revision of the sensor's sampling algorithm was thus needed since extensive manual editing of the salinity records as done in SPURS-1 cannot be applied to the drifters' real-time data. After detailed testing, the salinity sensors of the SVP-S drifters deployed during the 2015 field experiment in the BoB were programmed as follows: Each drifter samples its SBE37-SI sensor for 30 measurements over 90 seconds before each five-minute (or later 30-minute) transmit cycle, with the sensor polled for instantaneous sampling. The median of the 30 samples is then transmitted along with additional statistical parameters such as kurtosis and skewness to facilitate recovery of the measured population (Figure 3a–c). While the kurtosis describes the “tailedness” or “peakedness” of each 30-sample population, the skewness is a measure of its asymmetry. A fresh bias as observed in SPURS-1 would thus be associated with values significantly different from that of a normal distribution, and necessary corrections could be implemented at an early stage. The example shown in Figure 3 is representative of all deployed SVP-S drifters, indicating along-track statistics close to a normal distribution and hence creating confidence in the revised sensor algorithm.

The tightly deployed array, and particularly the clusters that included three SVP-S drifters, allow for salinity intercomparisons of different sensors for validation purposes. Inspection of the individual salinity measurements in the context of nearby drifters shows overall good agreement during the first deployment month, despite the large spatiotemporal variability in the northern BoB due to rain squalls and river runoff (Figure 3d–f). In particular, the confirmation of freshening events by nearby drifters gives further confidence in the measured salinities. After about nine months, nearly all of the deployed drifters have stopped transmitting—mainly as a result of frequent pickups or grounding at the coast.

MULTISCALE VARIABILITY

To highlight the observed variability on multiple spatial and temporal scales in the northern BoB during the waning 2015 southwest monsoon, Figure 4 shows drifter speed as well as salinity and temperature. Although during the first month of deployment the drifters largely followed a mesoscale feature centered at about 16.5°N, 89°E (cf. Figure 1b), within which hydrographic properties were generally rather homogenous, pronounced salinity fluctuations are found at the periphery or outside of the cyclonic eddy. Maximum speeds of up to approximately 70 cm s⁻¹ are observed between about 16.5°N and 17.5°N and west of 88°E, where drifters

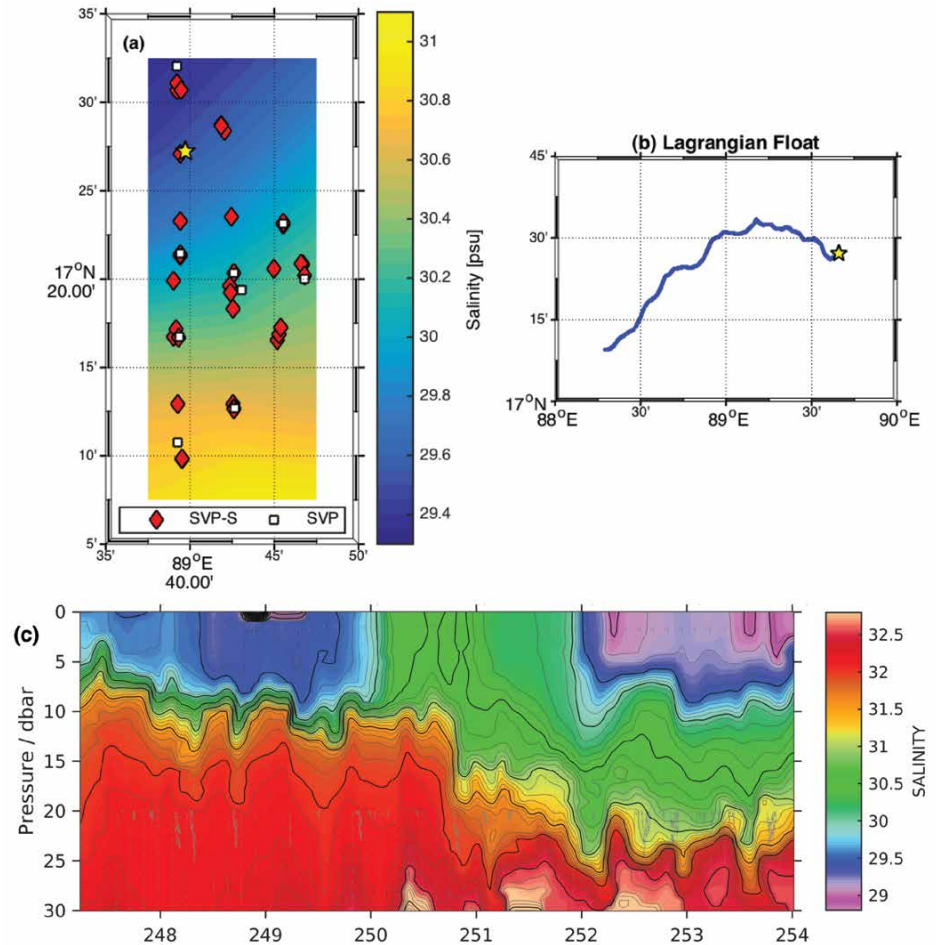


FIGURE 2. (a) Deployment locations of the SVP-S (red) and SVP (white) drifters in the northern Bay of Bengal at the beginning of September 2015, superimposed on the mapped initial salinities from the SVP-S drifters; note that the drifter array was deployed across a freshwater front. The yellow star marks the deployment location of a Lagrangian float whose trajectory is displayed in (b). The measured salinity distribution of the Lagrangian float in the upper 30 m of the water column is shown in (c), with x-axis in year days where 248 corresponds to September 5, 2015.

leave the eddy, as well as at its southern periphery; note that there is also evidence of near-inertial oscillations in the drifter tracks, particularly in the northeast of the sampled region as highlighted in Figure 5a,b. At the surface, the eddy can overall be characterized by temperatures and salinities of around 29°C and 30 psu, respectively, with fresher values toward the west (Figure 4b,c). Outside

of this mesoscale feature, the drifters show a warmer but patchy temperature field and lowest salinities of the order of 22 psu in the northwest toward the coastline (Figure 3a,d).

The measurements recorded by the Lagrangian float (Figure 2c) as well as data collected from conductivity-temperature-depth casts and other instruments during R/V *Roger Revelle*

and OSV *Sagar Nidhi* cruises suggest that the thickness of the near-surface freshwater layer in the salinity front region, where the drifters were initially deployed, can be less than 15 m. This prevented fully exploiting the Lagrangian information from the drifters at the beginning of the experiment since the drogue and salinity sensor are at different depths.

During the first week of the drifter deployment, several low-salinity patches were observed, similar to the ones shown in Figure 3e,f, with the persistence of the fresh patches varying from one hour to more than 24 hours. While the drifters remained trapped within or slipped through these patches, they covered distances over ground ranging from a few hundred meters to tens of kilometers (not shown); note that the actual cause of the sampled freshwater feature (e.g., short rain squall) may have played a role in these observations. Some of the observed salinity patches had amplitudes in excess of 1.5 psu (Figure 3f) and can be attributed to either direct freshwater input into the ocean from rain at the time of the salinity measurements or to the drifters entering and sampling a filament of freshwater that resulted from stirring processes near the salinity front or that was a remnant of a rain puddle. For example, the comparison between drifter salinities and rain rate shown in Figure 5c indicates that the salinity spikes around September 6, 2015, are most likely associated with a rain event whereas the prominent drop toward the end of the record is not.

While a truly Lagrangian analysis of the spatial and temporal scales cannot be performed with confidence, the salinity observations from the drifters can still be used in a Eulerian sense. To particularly quantify small spatiotemporal scales of the initial freshwater front, spatial autocorrelations of the drifter salinities expressed as Moran's I (Moran, 1950) were computed for 5 km \times 5 km spatial boxes and six-hour temporal windows over the first two days after completing the deployments (Figure 6). The boxes

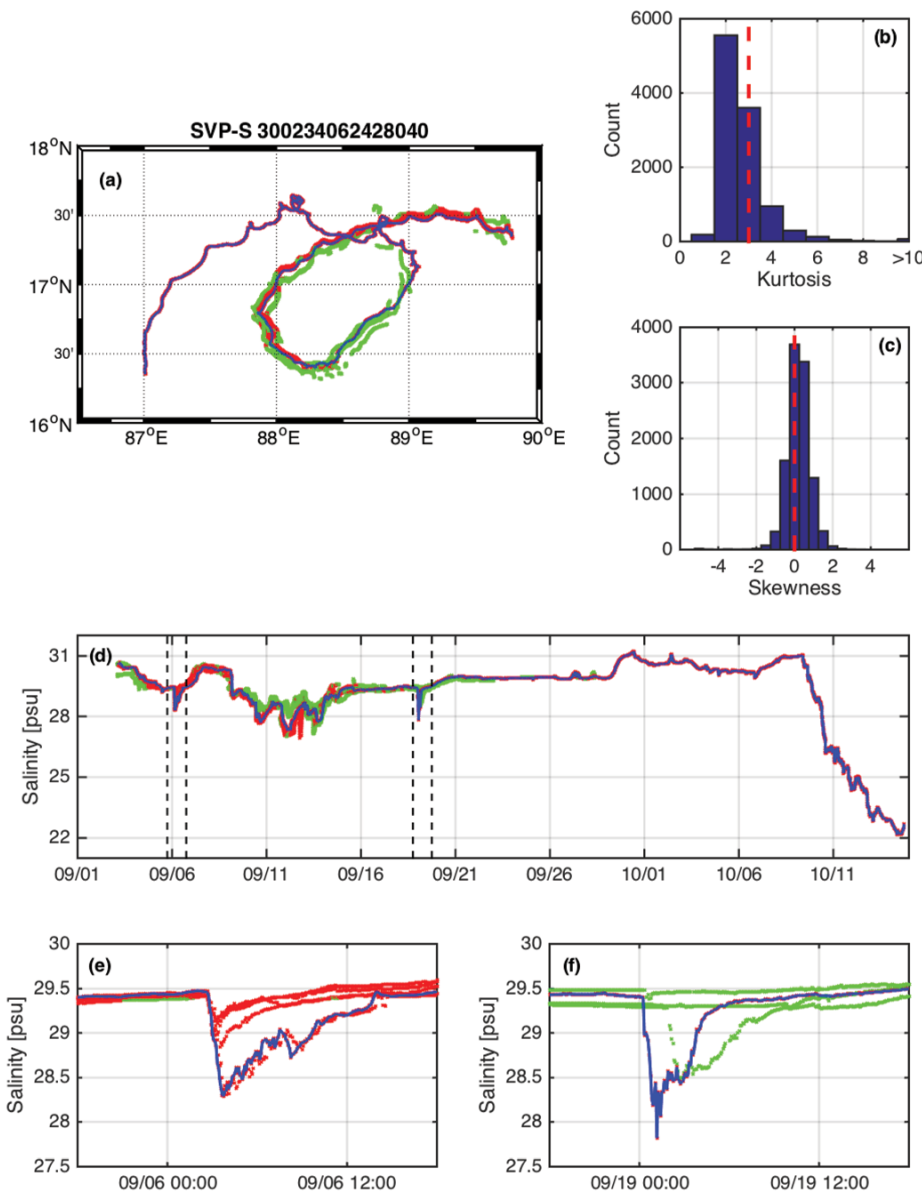


FIGURE 3. (a) Track of an SVP-S drifter (ID: 300234062428040) deployed on September 3, 2015 (blue), with locations of nearby drifters separated in time by ± 90 minutes and within 10 km (5 km) marked in green (red). Corresponding along-track SVP-S (b) kurtosis (i.e., “tailedness” or “peakedness” of the sample population; red dashed line indicates value for normal distribution) and (c) skewness (i.e., asymmetry of the sample population; red dashed line indicates 0) as statistical performance measures. (d) Quality-controlled salinity record of the SVP-S drifter (blue) and values measured by the nearby drifters as marked in (a); black dashed lines indicate two specific events shown in more detail in (e) and (f).

and windows were chosen according to the observed small-scale variability and persistence of fresh events such as those shown in Figure 3e,f. This approach highlights the short-lived character of freshwater features in the northern BoB on scales that are not well represented in numerical models.

Moran's I is based on cross products of deviations from the mean and can be calculated for n observations of a variable x (here, salinity) at locations i, j as follows:

$$I = \frac{n}{S_0} \frac{\sum_i \sum_j w_{ij} (x_i - \bar{x})(x_j - \bar{x})}{\sum_i (x_i - \bar{x})^2}, \quad (1)$$

where \bar{x} is the mean of the variable x , w_{ij} is the weight matrix (here, proportional to inverse distance of concurrent—that is, within six hours—salinity pairs), and $S_0 = \sum_i \sum_j w_{ij}$ is the sum of the elements of the weight matrix. To analyze spatial autocorrelations, a distance measure for two nearby observations must be defined to describe the relationship between sample locations; it is expressed as a weight matrix. Similar to a one-dimensional correlation coefficient, Moran's I describes the multidimensional correlation of a signal with nearby locations in space and generally ranges from -1 to $+1$ (note, only positive values were found here). That is, positive (negative) spatial autocorrelation means that similar (dissimilar) values occur close to each other or, in other words, Moran's I is an indication of whether the observations are clustered ($I = +1$), random ($I = 0$), or dispersed ($I = -1$); to ensure statistical significance, the spatial autocorrelations were computed only for boxes with more than 30 salinity pairs.

At the beginning, the drifters indicate some positive autocorrelation in the frontal region with common values between 0.4 and 0.7 (Figure 6a). As the drifters start to disperse over the next six hours, consistent autocorrelations of the order of 0.5 are found on the fresher side of the front while lower values and more pronounced salinity patchiness are observed in the northeast sector (Figure 6b). On September 4, 2015, the freshwater front begins to weaken (or the drifters slip through it), and the derived autocorrelations become more patchy (Figure 6c,d). The salinities in the region are generally lower after the disintegration or advection of the front past the drifters (i.e., ~ 29.5 psu), and a coherent pattern of spatial autocorrelations with, again, values of the order of 0.5, emerges around midday (Figure 6e). The following 12 hours partly show high spatial autocorrelations of more than 0.7 (Figure 6f,g), which drop back to common values of around 0.5 on September 5, 2015, at 6:00 (± 3 h) UTC (Figure 6h). The last

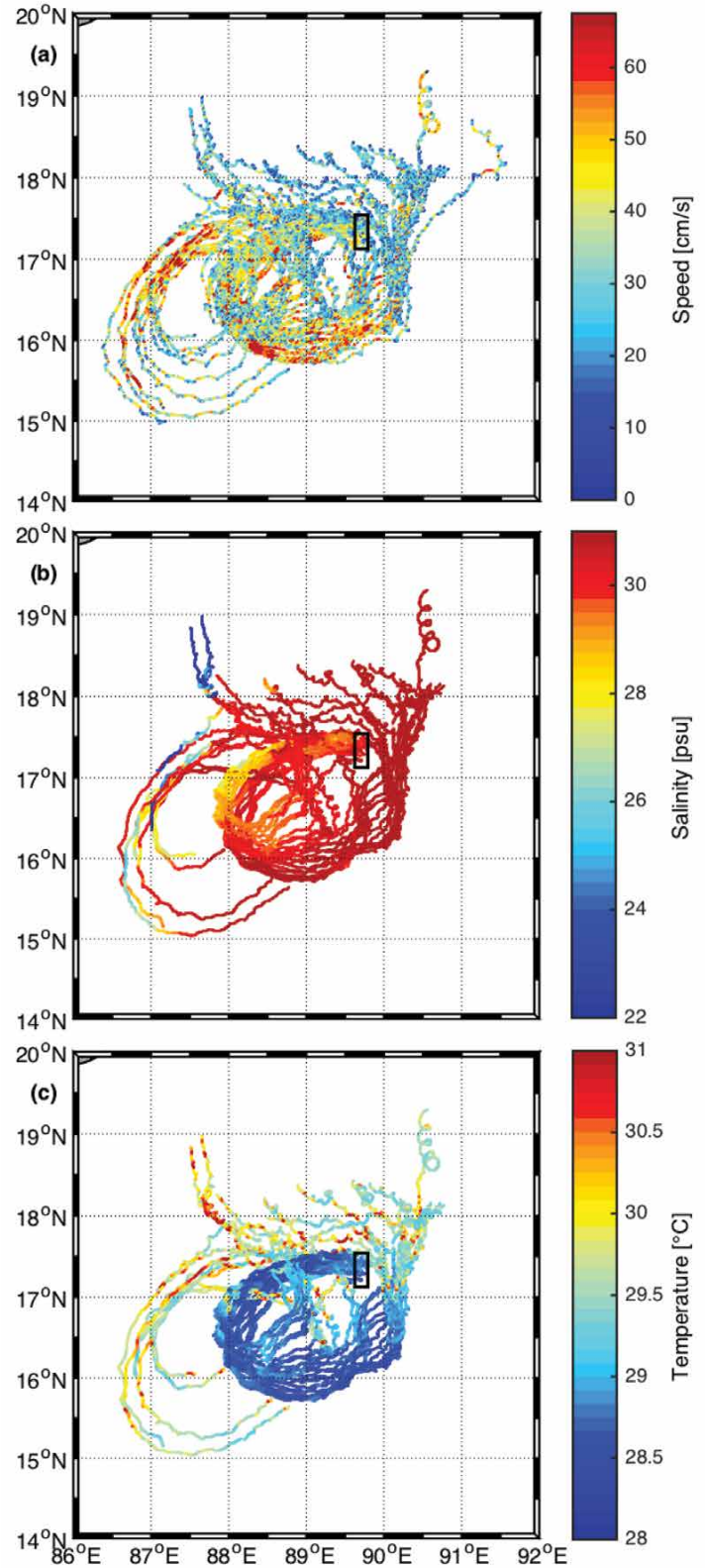


FIGURE 4. Trajectories of the deployed drifters color-coded by their (a) speed as well as (b) salinity and (c) temperature as recorded by the SBE37-SI sensor highlight the large variability that occurs on multiple spatial and temporal scales in the northern BoB. The black box marks the drifter deployment region.

snapshot in time indicates that the drifters enter a new salinity front or re-enter the previous one toward the southwest, with generally larger spatial autocorrelations on the fresher side (Figure 6i). Note overall that lower values of Moran's I may be related to filaments or rain puddles with scales of less than 5 km. This autocorrelation analysis not only presents a view of the involved spatial scales of the regional surface salinity but also illustrates the associated large variability in time as seen in the rapid evolution of freshwater fronts.

KINEMATIC PROPERTIES

The drifter deployment in clusters further permits insights into important kinematic properties of the observed Lagrangian velocities. In particular, first estimates of the vertical component of the vorticity vector, the horizontal divergence, and the lateral strain rate were derived from drifter triplets (e.g., Saucier, 1955; Molinari and Kirwan, 1975). The spatiotemporal distributions of the kinematic properties shed light on the processes that govern BoB dynamics, which were characterized by a strong mesoscale

eddy, pronounced fronts, and shallow salinity stratification during the deployment period, as discussed above. In the following, we examine the footprints of these features in the Lagrangian drifter velocities and their gradients.

By utilizing clusters of three (or more) drifters, the horizontal gradient of the velocity field can be estimated unambiguously (Kirwan, 1975). This study uses the planimetric method by Saucier (1955), originally devised for clusters of atmospheric wind reports, to estimate area-averaged components of the deformation tensor.

The divergence of the velocity field D can be interpreted as the time rate of change of the area enclosed by three drifters. A_0 and A' are the area enclosed by the drifters before and after being advected by the velocity field (u, v) for a time Δt :

$$\delta = \frac{\partial u}{\partial x} + \frac{\partial v}{\partial y} \approx \frac{A' - A_0}{A_0 \Delta t}. \quad (2)$$

When transforming the expression for the vorticity ζ into the horizontal divergence of the -90° -rotated velocity vectors, $(u', v') \rightarrow (v, -u)$, the same argument as above holds and the vorticity can be rewritten as the time rate of change of the cluster area:

$$\zeta = \frac{\partial v}{\partial x} - \frac{\partial u}{\partial y} \rightarrow \frac{\partial u'}{\partial x} + \frac{\partial v'}{\partial y} \approx \frac{A'' - A_0}{A_0 \Delta t}, \quad (3)$$

where A'' is the cluster area after being subjected to the rotated velocity field for a time Δt .

Similarly, the shearing and stretching deformations can be estimated by evaluating the divergence of the rotated velocity fields. The velocity fields are rotated such that $(u'', v'') \rightarrow (u, -v)$ and $(u''', v''') \rightarrow (v, u)$ for the shearing and stretching components, respectively. The magnitude of the lateral strain rate α is computed from the stretching and shearing rates as follows (e.g., Saucier, 1955; Shcherbina et al., 2013):

$$\alpha = \sqrt{\left(\frac{\partial u}{\partial x} - \frac{\partial v}{\partial y}\right)^2 + \left(\frac{\partial v}{\partial x} + \frac{\partial u}{\partial y}\right)^2}. \quad (4)$$

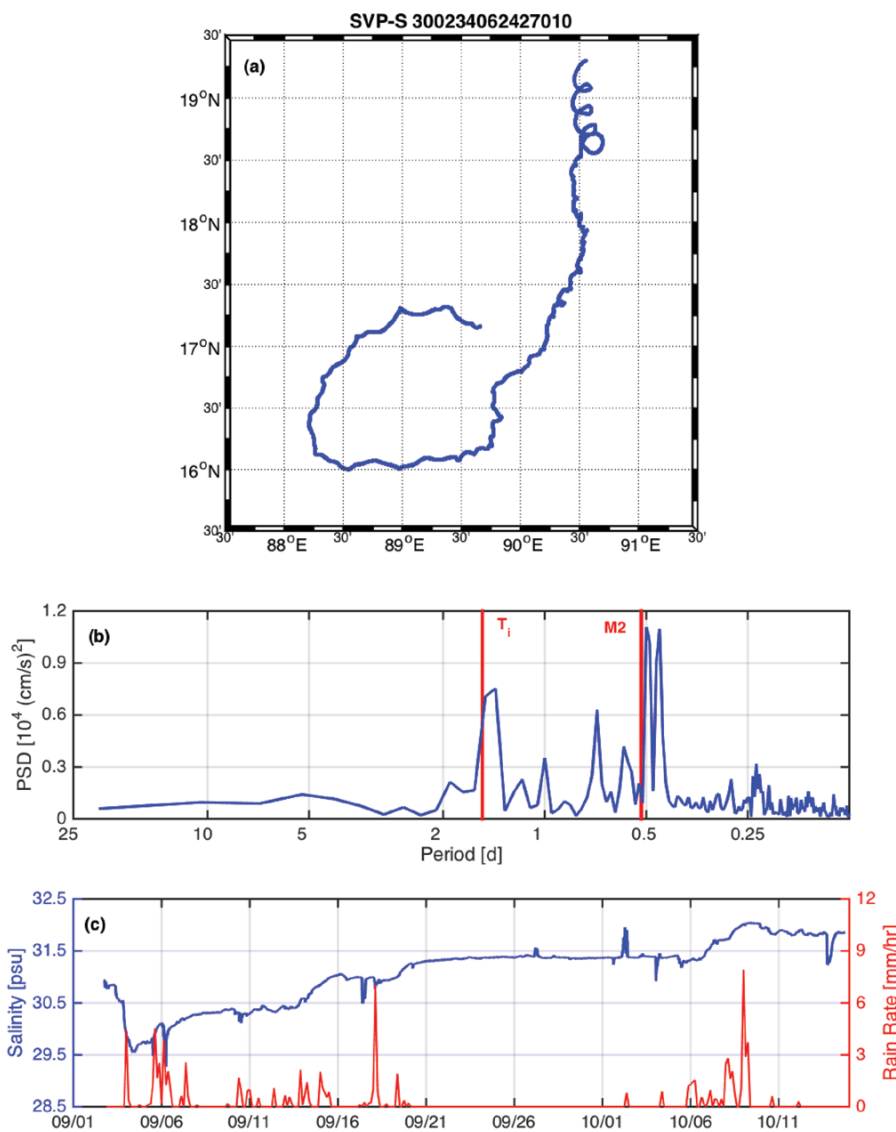


FIGURE 5. (a) Track of an SVP-S drifter (ID: 300234062427010) deployed on September 2, 2015. (b) Variance-conserving power spectrum of the drifter's speed, with the local inertial period T_1 at 19°N and the M2 tide marked by red lines. (c) Quality-controlled salinity record of the SVP-S drifter (blue) and corresponding Tropical Rainfall Measuring Mission (TRMM) 3B42 rain rate (Huffman et al., 2007) mapped onto the drifter's track (red).

The scale dependence of the area averages is exploited in order to separate processes at different scales (Figure 7). When averaging over large areas ($A > 100 \text{ km}^2$), the small-scale variability is smoothed and the strong mesoscale eddy dominates the vorticity, strain, and divergence distributions (not shown). In this case, the vorticity and strain are of the same order of magnitude of about $0.5 f$. At intermediate scales ($10 \leq A \leq 100 \text{ km}^2$), a range of processes, including at the mesoscale, affect the distribution of the kinematic properties (Figure 7a,c,e). Besides the mesoscale circulation, submesoscale dynamics tend to cause regions of high vorticity and strain to co-occur (e.g., Shcherbina et al., 2013). Since anticyclonic features become unstable faster than cyclonic ones, the resulting distribution is skewed toward longer tails for cyclonic vorticity (not shown). Furthermore, it is expected that frontogenesis has a signature in the horizontal divergence, and small cluster areas lead to large values in the kinematic properties at submesoscales ($A < 10 \text{ km}^2$; Figure 7b,d,f).

The derived kinematic properties from the drifter clusters complement the information gained by their temperature and salinity measurements at the surface. However, more work is needed to link the observed small-scale variability in the kinematic properties to the hydrographic observations.

SUMMARY AND DISCUSSION

A dedicated drifter experiment was conducted in the northern BoB during the 2015 waning southwest monsoon (Figure 1a). To sample a variety of spatiotemporal scales and particularly the horizontal advection of freshwater, the deployment was designed as a tight array largely organized in clusters of three SVP-S drifters plus one SVP drifter (Figure 2a). After discovering a flaw in the algorithm used for the onboard computation of satellite-transmitted drifter salinities during SPURS-1 (Centurioni et al., 2015; Hormann et al., 2015), the sensor

algorithm was revised for the SVP-S drifters described here, and its first evaluations in the northern BoB (Figure 3) are very encouraging for future experiments such as SPURS-2 in the eastern equatorial Pacific (SPURS-2 Planning Group, 2015).

Following their deployment, most of the drifters were quickly entrained in a mesoscale feature centered at about 16.5°N , 89°E (Figure 1b) and stayed close together during the first month of observations. While the eddy was associated with rather homogeneous temperature and salinity characteristics, much larger variability was found outside of it toward the coastline (Figure 4), and some of the observed salinity patches had amplitudes in excess of 1.5 psu (Figure 3f). The drifters further indicated that near-inertial oscillations may be of

importance for the observed salinity variability, in particular toward the northern coastline (Figure 5a,b). In order to particularly quantify the smaller spatiotemporal scales, an autocorrelation analysis of the drifter salinities for the first two days after completing the deployments was performed; it indicated not only spatial scales of less than 5 km but also temporal variations of the order of a few hours (Figure 6).

By deploying the drifters in clusters, important kinematic properties (i.e., vorticity, strain, and divergence) during the 2015 waning southwest monsoon could be estimated (Figure 7), providing new perspectives on the processes driving upper-ocean salinity variability in the BoB in particular. Although the kinematic properties derived from the drifter

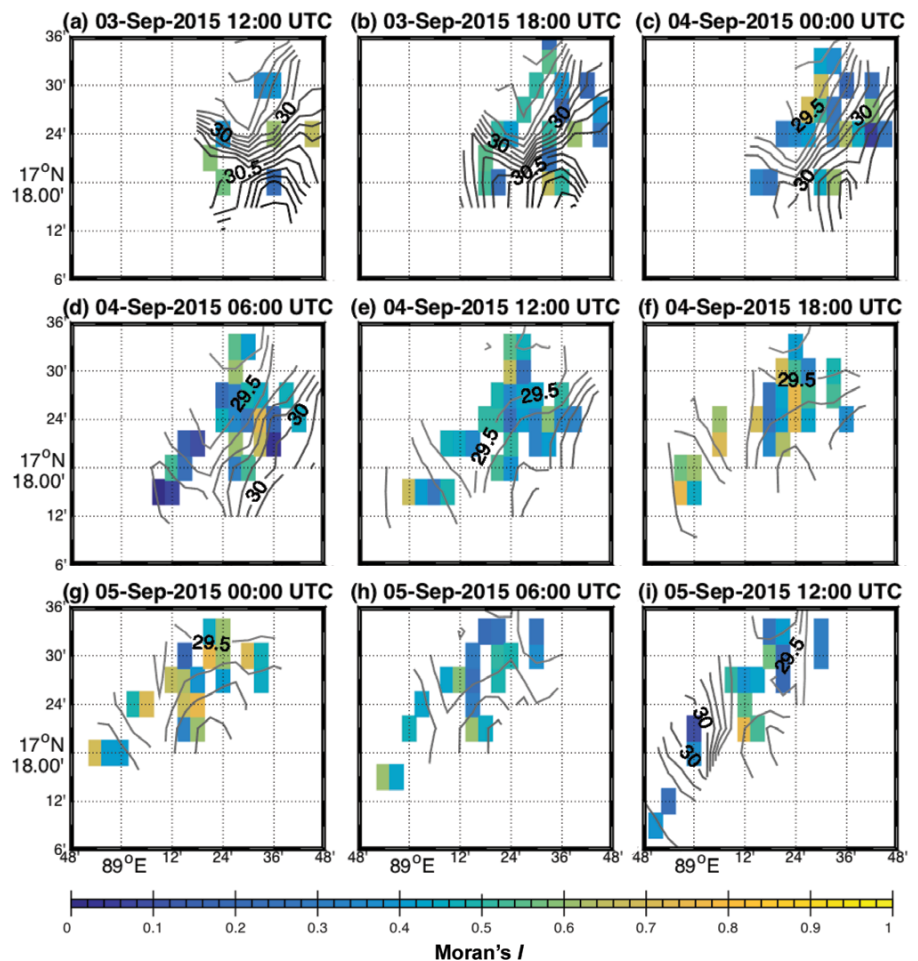



FIGURE 6. Spatial autocorrelations of the drifter salinities expressed as Moran's I for the first two days after completing the deployments using $5 \text{ km} \times 5 \text{ km}$ spatial boxes and six-hour temporal windows. Frontal salinity gradients as derived from mapping of the SVP-S data are indicated by superimposed grayscale contours in intervals of 0.1 psu .

array could be used to resolve processes at different scales, more work is needed to link the observed characteristics to the hydrographic measurements.

Since the SVP-S drifters concurrently measure salinity and velocity, they can be used to quantify the divergence of the

salt fluxes in the BoB (e.g., Centurioni et al., 2015), and corresponding analyses are underway. However, the mixed layers in the northern bay can be very shallow as observed during the 2015 ASIRI field campaign (Figure 2c). They can be at less than 15 m depth, resulting

in drifter velocities below the mixed layer, but salinity measurements within it (i.e., SBE37-SI at 0.5 m). These observations need to be taken into account in order to obtain meaningful flux estimates from the drifters that can be compared with other evaluations. 

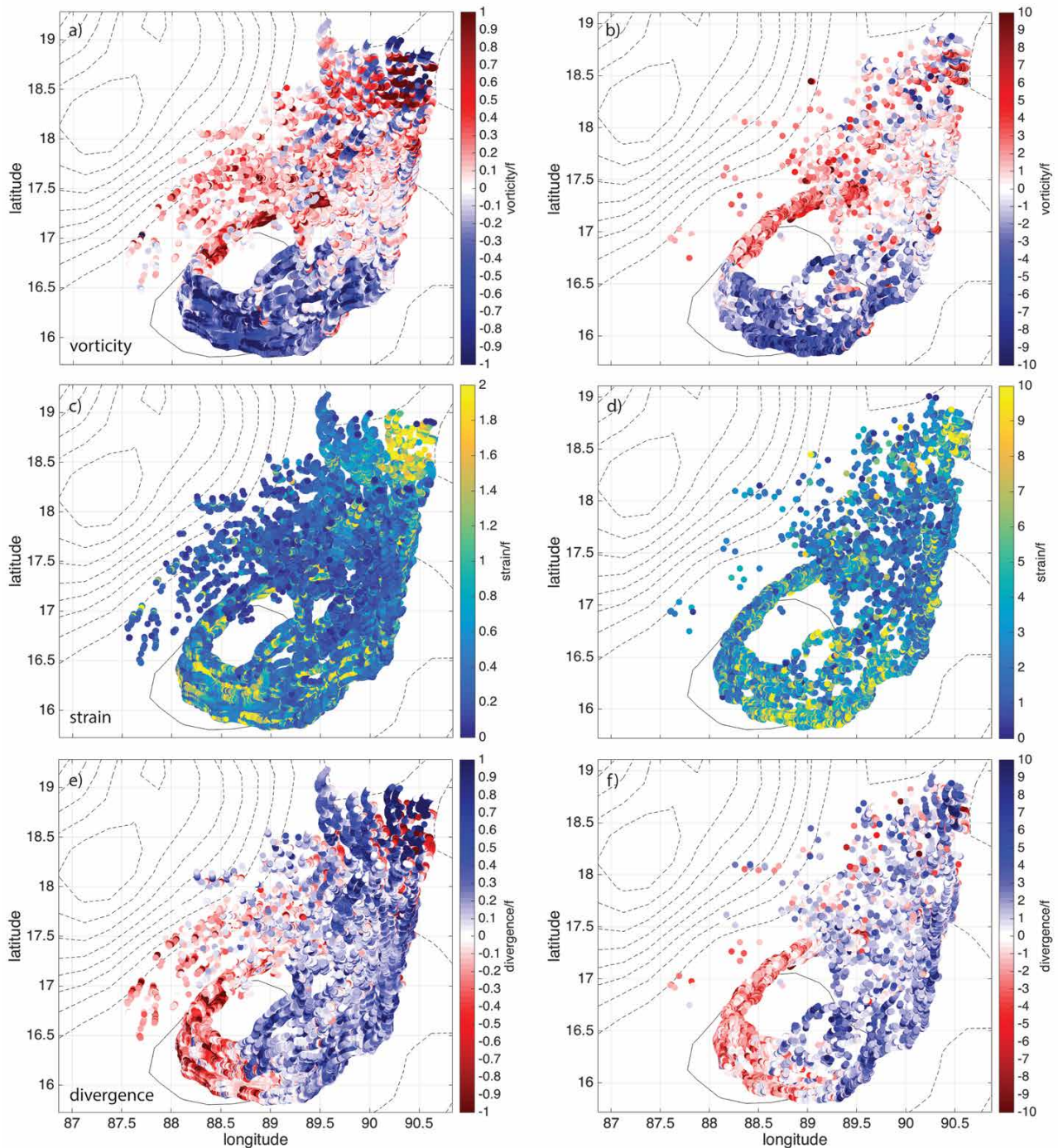


FIGURE 7. Maps of (a,b) vorticity ζ , (c,d) lateral strain rate α , and (e,f) horizontal divergence δ , all normalized by f , averaged over two different area ranges during the first month of deployment. The left column (a,c,e) shows kinematic properties averaged over an area of $10 \leq A \leq 100 \text{ km}^2$, while the right column (b,d,f) is averaged over an area of $1 < A < 10 \text{ km}^2$. Contours of sea level anomalies from CMEMS (Ducet et al., 2000) are shown in the background, with negative (positive) values indicated by dashed (solid) lines.

REFERENCES

- Bhat, G.S., S. Gadgil, P.V. Hareesh Kumar, S.R. Kalsi, P. Madhusoodanan, V.S.N. Murty, C.V.K. Prasada Rao, V. Ramesh Babu, L.V.G. Rao, R.R. Rao, and others. 2001. BOBMEX: The Bay of Bengal Monsoon Experiment. *Bulletin of the American Meteorological Society* 82:2,217–2,243, [http://dx.doi.org/10.1175/1520-0477\(2001\)082<2217:BTBOBM>2.0.CO;2](http://dx.doi.org/10.1175/1520-0477(2001)082<2217:BTBOBM>2.0.CO;2).
- Centurioni, L.R., V. Hormann, Y. Chao, G. Reverdin, J. Font, and D.-K. Lee. 2015. Sea surface salinity observations with Lagrangian drifters in the tropical North Atlantic during SPURS: Circulation, fluxes, and comparisons with remotely sensed salinity from Aquarius. *Oceanography* 28:96–105, <http://dx.doi.org/10.5670/oceanog.2015.08>.
- D'Asaro, E. 2003. Performance of autonomous Lagrangian floats. *Journal of Atmospheric and Oceanic Technology* 20:896–911, [http://dx.doi.org/10.1175/1520-0426\(2003\)020<0896:POALF>2.0.CO;2](http://dx.doi.org/10.1175/1520-0426(2003)020<0896:POALF>2.0.CO;2).
- Dee, D.P., S.M. Uppala, A.J. Simmons, P. Berrisford, P. Poli, S. Kobayashi, U. Andrae, M.A. Balmaseda, G. Balsamo, P. Bauer, and others. 2011. The ERA-Interim reanalysis: Configuration and performance of the data assimilation system. *Quarterly Journal of the Royal Meteorological Society* 137:553–597, <http://dx.doi.org/10.1002/qj.828>.
- Ducet, N., P.Y. Le Traon, and G. Reverdin. 2000. Global high-resolution mapping of ocean circulation from TOPEX/Poseidon and ERS-1 and -2. *Journal of Geophysical Research* 105(C8):19,477–19,498, <http://dx.doi.org/10.1029/2000JC900063>.
- Gadgil, S. 2003. The Indian monsoon and its variability. *Annual Review of Earth and Planetary Sciences* 31:429–467, <http://dx.doi.org/10.1146/annurev.earth.31.100901.141251>.
- Hormann, V., L.R. Centurioni, and G. Reverdin. 2015. Evaluation of drifter salinities in the subtropical North Atlantic. *Journal of Atmospheric and Oceanic Technology* 32:185–192, <http://dx.doi.org/10.1175/JTECH-D-14-00179.1>.
- Huffman, G.J., R.F. Adler, D.T. Bolvin, G. Gu, E.J. Nelkin, K.P. Bowman, Y. Hong, E.F. Stocker, and D.B. Wolff. 2007. The TRMM multi-satellite precipitation analysis: Quasi-global, multiyear, combined-sensor precipitation estimates at fine scales. *Journal of Hydrometeorology* 8:38–55, <http://dx.doi.org/10.1175/JHM560.1>.
- Kirwan, A.D. Jr. 1975. Oceanic velocity gradients. *Journal of Physical Oceanography* 5:729–735, [http://dx.doi.org/10.1175/1520-0485\(1975\)005<0729:OVG>2.0.CO;2](http://dx.doi.org/10.1175/1520-0485(1975)005<0729:OVG>2.0.CO;2).
- Lee, C.M., S.U.P. Jinadasa, A. Anutaliya, L.R. Centurioni, H.J.S. Fernando, V. Hormann, M. Lankhorst, L. Rainville, U. Send, and H.W. Wijesekera. 2016. Collaborative observations of boundary currents, water mass variability, and monsoon response in the southern Bay of Bengal. *Oceanography* 29(2):102–111, <http://dx.doi.org/10.5670/oceanog.2016.43>.
- Lucas, A.J., E.L. Shroyer, H.W. Wijesekera, H.J.S. Fernando, E. D'Asaro, M. Ravichandran, S.U.P. Jinadasa, J.A. MacKinnon, J.D. Nash, R. Sharma, and others. 2014. Mixing to monsoons: Air-sea interactions in the Bay of Bengal. *Eos, Transactions American Geophysical Union* 95:269–270, <http://dx.doi.org/10.1002/2014EO300001>.
- Maximenko, N., R. Lumpkin, and L. Centurioni. 2013. Ocean surface circulation. Pp. 283–304 in *Ocean Circulation and Climate: A 21st Century Perspective*. G. Siedler, S.M. Griffies, J. Gould, and J.A. Church, eds, Academic Press.
- Molinari, R., and A.D. Kirwan Jr. 1975. Calculations of differential kinematic properties from Lagrangian observations in the western Caribbean Sea. *Journal of Physical Oceanography* 5:483–491, [http://dx.doi.org/10.1175/1520-0485\(1975\)005<0483:CODKPF>2.0.CO;2](http://dx.doi.org/10.1175/1520-0485(1975)005<0483:CODKPF>2.0.CO;2).
- Moran, P.A.P. 1950. Notes on continuous stochastic phenomena. *Biometrika* 37:17–23, <http://dx.doi.org/10.2307/2332142>.
- Niiler, P. 2001. The world ocean surface circulation. Pp. 193–204 in *Ocean Circulation and Climate*. G. Siedler, J. Church, and J. Gould, eds, Academic Press.
- Rao, R.R., and R. Sivakumar. 2003. Seasonal variability of sea surface salinity and salt budget of the mixed layer of the north Indian Ocean. *Journal of Geophysical Research* 108(C1), 3009, <http://dx.doi.org/10.1029/2001JC000907>.
- Reverdin, G., P. Blouch, J. Boutin, P.P. Niiler, J. Rolland, W. Scuba, A. Lourenco, and A.F. Rios. 2007. Surface salinity measurements: COSMOS 2005 experiment in the Bay of Biscay. *Journal of Atmospheric and Oceanic Technology* 24:1,643–1,654, <http://dx.doi.org/10.1175/JTECH2079.1>.
- Saucier, W.J. 1955. *Principles of Meteorological Analysis*. University of Chicago Press, 438 pp.
- Schott, F.A., and J.P. McCreary Jr. 2001. The monsoon circulation of the Indian Ocean. *Progress in Oceanography* 51:1–123, [http://dx.doi.org/10.1016/S0079-6611\(01\)00083-0](http://dx.doi.org/10.1016/S0079-6611(01)00083-0).
- Shcherbina, A.Y., E.A. D'Asaro, C.M. Lee, J.M. Klymak, M.J. Molemaker, and J.C. McWilliams. 2013. Statistics of vertical vorticity, divergence, and strain in a developed submesoscale turbulence field. *Geophysical Research Letters* 40(1):4,706–4,711, <http://dx.doi.org/10.1002/grl.50919>.
- Shenoi, S.S.C., D. Shankar, and S.R. Shetye. 2002. Differences in heat budgets of the near-surface Arabian Sea and Bay of Bengal: Implications for the summer monsoon. *Journal of Geophysical Research* 107(C6), 3052, <http://dx.doi.org/10.1029/2000JC000679>.
- SPURS-2 Planning Group. 2015. From salty to fresh—Salinity Processes in the Upper-ocean Regional Study-2. *Oceanography* 28(1):150–159, <http://dx.doi.org/10.5670/oceanog.2015.15>.
- Wang, B., and Z. Fan. 1999. Choice of South Asian summer monsoon indices. *Bulletin of the American Meteorological Society* 80:629–638, [http://dx.doi.org/10.1175/1520-0477\(1999\)080<0629:COSASM>2.0.CO;2](http://dx.doi.org/10.1175/1520-0477(1999)080<0629:COSASM>2.0.CO;2).
- Wang, B., R. Wu, and K.-M. Lau. 2001. Interannual variability of the Asian summer monsoon: Contrasts between the Indian and the western North Pacific-East Asian monsoons. *Journal of Climate* 14:4,073–4,090, [http://dx.doi.org/10.1175/1520-0442\(2001\)014<4073:IVOTAS>2.0.CO;2](http://dx.doi.org/10.1175/1520-0442(2001)014<4073:IVOTAS>2.0.CO;2).
- Wijesekera, H.W., T.G. Jensen, E. Jarosz, W.J. Teague, E.J. Metzger, D.W. Wang, S.U.P. Jinadasa, K. Arulananthan, L.R. Centurioni, and H.J.S. Fernando. 2015. Southern Bay of Bengal currents and salinity intrusions during the northeast monsoon. *Journal of Geophysical Research* 120:6,897–6,913, <http://dx.doi.org/10.1002/2015JC010744>.
- Wijesekera, H.W., E. Shroyer, A. Tandon, M. Ravichandran, D. Sengupta, S.U.P. Jinadasa, H.J.S. Fernando, N. Agarwal, K. Arulananthan, G.S. Bhat, and others. In press. ASIRI: An ocean-atmosphere initiative for Bay of Bengal. *Bulletin of the American Meteorological Society*, <http://dx.doi.org/10.1175/BAMS-D-14-00197.1>.

is INCOIS contribution number 247. Lance Braasch and Lance Curtiss are gratefully acknowledged for their efforts to improve the SVP-S drifters and assistance with the drifter data; specifically, the real-time distribution of SVP and SVP-S data implemented and managed by Lance Braasch was greatly appreciated during the 2015 field campaign. The master and crew of R/V *Roger Revelle* are thanked for making the drifter deployments possible, as well as two anonymous reviewers for their comments. Ssalto/Duacs altimeter products were produced and distributed by CMEMS (<http://www.marine.copernicus.eu>). The TRMM 3B42 data used in this effort were acquired as part of the activities of NASA's Science Mission Directorate (http://mirador.gsfc.nasa.gov/collections/TRMM_3B42_007.shtml), and are archived and distributed by the Goddard Earth Sciences Data and Information Services Center.

AUTHORS

Verena Hormann (vhormann@ucsd.edu) is Assistant Project Scientist and **Luca R. Centurioni** is Associate Researcher and Principal Investigator of the Global Drifter Program, both at Scripps Institution of Oceanography, University of California, San Diego, La Jolla, CA, USA. **Amala Mahadevan** is Senior Scientist, Woods Hole Oceanographic Institution, Woods Hole, MA, USA. **Sebastian Essink** is a graduate student in the MIT-WHOI Joint Program in Oceanography, Cambridge/Woods Hole, MA, USA. **Eric A. D'Asaro** is Senior Principal Oceanographer, Applied Physics Laboratory, and Professor, School of Oceanography, University of Washington, Seattle, WA, USA. **B. Praveen Kumar** is Scientist, Indian National Centre for Ocean Information Services, Hyderabad, India.

ARTICLE CITATION

Hormann, V., L.R. Centurioni, A. Mahadevan, S. Essink, E.A. D'Asaro, and B. Praveen Kumar. 2016. Variability of near-surface circulation and sea surface salinity observed from Lagrangian drifters in the northern Bay of Bengal during the waning 2015 southwest monsoon. *Oceanography* 29(2):124–133, <http://dx.doi.org/10.5670/oceanog.2016.45>.

ACKNOWLEDGMENTS

VH and LR were supported by ONR grant N00014-13-1-0477 and NOAA GDP grant NA10OAR4320156. AM and SE were funded by ONR grant N00014-13-1-0451, and ED by ONR grant N00014-14-1-0235. BPK acknowledges financial support from the Ministry of Earth Sciences (MoES, Government of India), and this